32nd Annual International Conference of the IEEE EMBS
Buenos Aires, Argentina, August 31 - September 4, 2010

Cell Micromanipulation with an Active Handheld Micromanipulator

Jaime Cuevas Tabarés, Robert A. MacLachlan, *Member, IEEE*, Charles A. Ettensohn, and Cameron N. Riviere, *Member, IEEE*

***Abstract*—The paper describes the use of an active handheld micromanipulator, known as Micron, for micromanipulation of cells. The device enables users to manipulate objects on the order of tens of microns in size, with the natural ease of use of a fully handheld tool. Micron senses its own position using a purpose-built microscale optical tracker, estimates the erroneous or undesired component of hand motion, and actively corrects it by deflecting its own tool tip using piezoelectric actuators. Benchtop experiments in tip positioning show that active compensation can reduce positioning error by up to 51% compared to unaided performance. Preliminary experiments in bisection of sea urchin embryos exhibit an increased success rate when performed with the help of Micron.**

I. Introduction

Biological sciences and technology rely heavily on cell manipulation techniques [1]. Numerous advanced technologies have been proposed for this problem, including electrophoresis and dielectrophoresis [2], microfluidic manipulation [3], and ferromagnetic microtransporters [4]. Meanwhile, freehand techniques are used for certain cell micromanipulation tasks, despite the attendant difficulty, due to the need for high dexterity [5]. We propose that for certain kinds of cell micromanipulation there may be advantages to using an active handheld micromanipulator known as Micron. This tool actively compensates for the user's hand tremor, making it possible to manipulate objects in the order of tens of micrometers while preserving the ease of use of a freehand tool. Ref. [6] describes the use of an earlier version of Micron in conjunction with computer vision for eye microsurgery. Here we describe the core Micron system (without computer vision), and use a newer version of Micron that has higher performance due to improvements in manipulator fabrication and control algorithms, and report preliminary results in bench-top positioning tests and in cell micromanipulation.

II. System Design

Fig. 1 shows the current Micron system, which operates using closed-loop optical position measurement. The operator freely manipulates the handpiece just like a conventional tool, subject only to the constraint that the tracking LEDs remain visible to the position sensor (PSD cameras). Micron can be used with any appropriate conventional microscope; no hardware integration is required. A laser finder on the cameras aids sensor alignment so that the 4 cm workspace can be centered at the desired handpiece location.

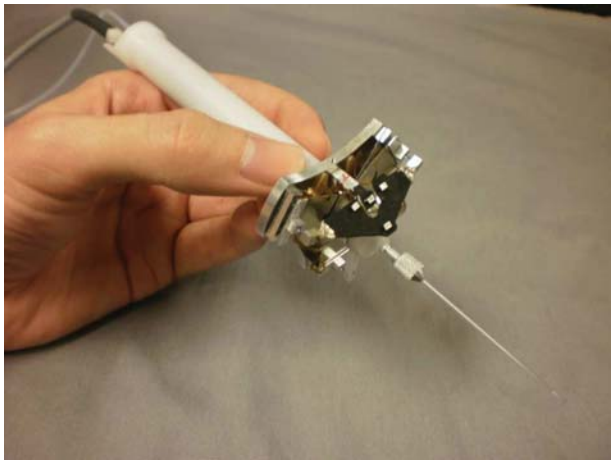

Fig. 1. The Micron handpiece, with the housing removed.

Fig. 2 is a block diagram of the system. Optical measurement determines the six-degree-of-freedom pose of the handgrip and tool using one LED fixed to the handle and three LEDs coupled to the tool mount. A feedback loop running at 2 kHz servos the tool tip to the desired position,

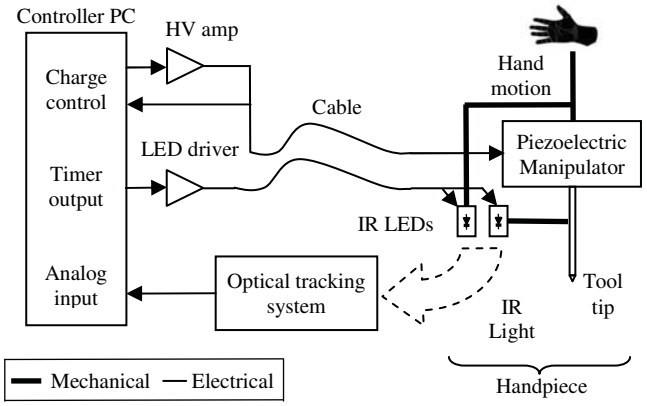

Fig. 2. Micron structure. The manipulator and the LEDs are attached to the handpiece. The controller PC receives position feedback and controls the manipulator through an electronic interface.

This work was supported in part by the U.S. National Institutes of Health under Grants R01 EB000526, R21 EY016359, and R01 EB007969.

J. Cuevas Tabarés is with the University of Valladolid, Spain.

R. A. MacLachlan, and C. N. Riviere are with the Robotics Institute, Carnegie Mellon University, Pittsburgh, PA 15213 USA (e-mail: camr@ri.cmu.edu).

C. A. Ettensohn is with the Dept. of Biological Sciences, Carnegie Mellon University, Pittsburgh, PA 15213 USA.

rejecting disturbance by hand tremor and manipulator error. Charge control is used to linearize the piezoelectric manipulator, greatly reducing hysteresis.

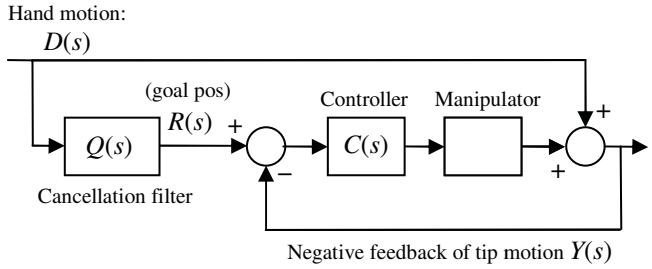

Fig. 3. Micron small-signal model with cancellation filter. Hand motion is measured and filtered to establish the goal position.

Low-latency, high-resolution position feedback is required for closed loop control of the high-bandwidth manipulator. The measurement subsystem optically tracks four LEDs at 2 kHz with 3 um resolution over a 4-cm workspace [7]. The Position Sensitive Detector (PSD) cameras do not record an image; instead the sensors make a direct analog measurement of the centroid of a light source in two degrees of freedom. Multiple LEDs are tracked simultaneously using frequency domain multiplexing.

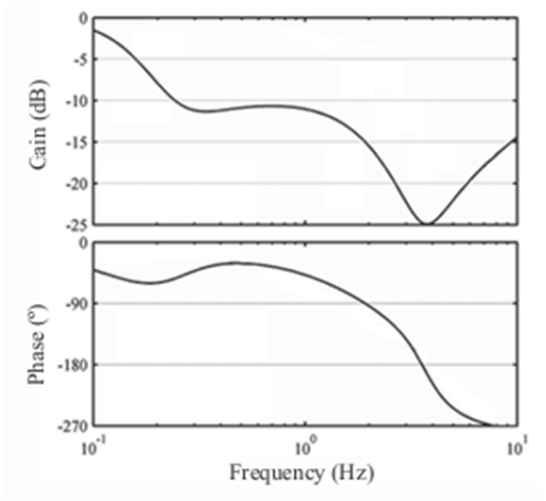

Fig. 4. Micron low-frequency response, hand to tip.

Fig. 3 is a small-signal model of Micron closed-loop operation. A position servo loop compares the measured tip position $Y(s)$ to the goal position $R(s)$. A controller $C(s)$ compensates for the manipulator dynamics $G(s)$ to command manipulator motion minimizing the position error. This motion is mechanically added to the hand motion disturbance $D(s)$, cancelling the undesired motion. This negative feedback cancels all hand motion. Voluntary control of the tool tip is preserved by making the goal $R(s)$ be a filtered version of the measured hand motion. The cancellation filter Q(s) has a generally low-pass response, since it must have unity gain at low frequencies so that the tip remains within the manipulator workspace in spite of gross hand motion, yet should suppress high-frequency tremor components. The filter requirements are defined both by the nature of tremor and the dynamics of the human operator. Excessive lag at the unity-gain crossover frequency of the eye-hand feedback loop (around 1 Hz [8]) destabilizes the overall system, resulting in a response that feels bouncy even though $Q(s)$ itself may have negligible overshoot; hence it is beneficial for the corner frequency to be set above 1 Hz, in order to preserve intuitive eye-hand coordination. Although this suppresses high-frequency tremor, the amplitude of tremor below 1 Hz is considerably greater [9].

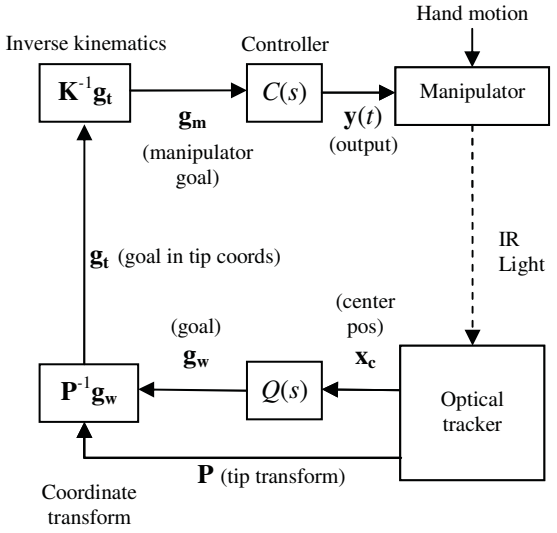

Fig. 5. Block diagram of the system to control the 3-DOF manipulator.

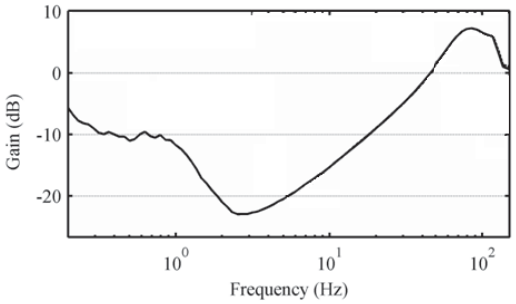

Fig. 6. Micron system closed-loop gain (hand to tip) with cancellation.

Motion scaling reduces the effect of low-frequency tremor by scaling down hand motion so that the operator makes larger motions with greater relative accuracy. Scaling preserves stability, since the flat frequency response need not introduce any significant delay. The Micron goal filter approximates motion scaling by implementing a shelving response. $Q(s)$ has a low corner frequency f_L, a flat shelf near 1 Hz with amplitude k_S (the scaling region), and then a high corner frequency f_H (above 1 Hz). From a control perspective, this can be seen as lead-lag compensation of the human feedback loop. Fig. 4 shows the frequency response of Micron with f_L = 0.15 Hz, f_H = 2 Hz, and k_S = 1/3. The parameters were empirically adjusted to obtain a balance between tremor cancellation, intuitive performance and manipulator range, as a low f_L or a high k_S cause saturation.

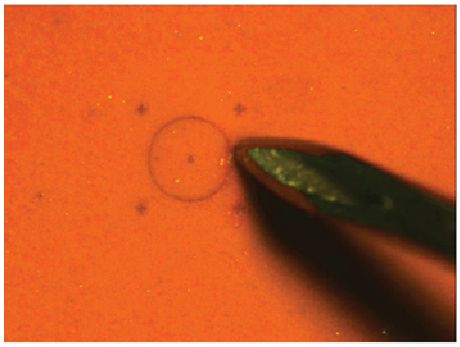

Fig. 7. Positioning tests workspace view.

The linear shelving filter is preceded by a nonlinear element: a 1 mm/s velocity limiter. Fig. 4 does not represent the effect of velocity limiting, which is amplitude-dependent. As long as the voluntary motion does not exceed the limit there is no destabilizing effect on eye-hand feedback.

The Micron software uses transform matrices to convert positions between three coordinate systems: world, tool tip, and manipulator joint space (Fig. 5). The LED positions are used to find tip pose **P** (a 4x4 linear homogenous transform matrix) and $\mathbf{x_c}$, the coordinates of the center of the workspace. Because $\mathbf{x_c}$ is where the tip would be in a conventional rigid tool, this point is passed through the cancellation filter $Q(s)$ to find the tip position goal in world coordinates, $\mathbf{g_w}$. Multiplying by the matrix inverse of the tip pose ($\mathbf{P}^{-1}\mathbf{g_w}$) transforms the goal position into the tip coordinate system, giving $\mathbf{g_t}$, an offset relative to the current tip position. This transform is analogous to the $R(s) - Y(s)$ node in the small-signal model (Fig. 3), so $\mathbf{g_t}$ plays the role of the error signal in the feedback loop. Since high frequencies have been removed from $\mathbf{g_w}$, this has the effect of passing forward the high frequency content in **P** with a negative sign, creating negative feedback at high frequencies. Recall that the manipulator is a 3-DOF parallel linkage. We convert the desired tip position into link lengths ($\mathbf{g_m}$) using the inverse kinematics transform $\mathbf{K}^{-1}\mathbf{g_t}$. Although the true inverse kinematics is nonlinear, due to the small angular deflection, a linear approximation works well. $C(s)$ is a PID controller followed by a notch filter (which compensates for the 175 Hz manipulator resonance). In comparison to the system in Ref. [6], the use of this notch filter permits higher feedback gains, improving tremor suppression.

The limited range of manipulator motion (covering a 400 um cube) complicates control because undesired motion often exceeds this range. Manipulator saturation causes two problems: first, as long as the manipulator is saturated, no cancellation can take place, and second, saturation opens the feedback loop, causing undesirable motion on the axes that are not saturated. Recently we have greatly reduced the severity of this problem by substituting a reachable compromise goal position when the desired goal position is unreachable. Another layer of saturation management adaptively increases the cutoff frequency of the cancellation filter $Q(s)$, gracefully avoiding saturation by compromising the cancellation filter attenuation when the manipulator nears saturation.

Fig. 6 shows the measured gain of the micron system, from handle to tip. At low frequencies the closed-loop response is very similar to the simulation in Fig. 4. Above 4 Hz until the unity gain crossover (near 60 Hz), the closed-loop attenuation is approximately equal to the open-loop gain. Near 100 Hz the gain increases to 6 dB (negative attenuation), which has little practical effect because there is negligible tremor at this frequency.

III. EXPERIMENTAL TESTING

Two sets of experiments were carried out in order to test the ability of Micron to perform cell micromanipulation tasks. The first set consisted in handheld positioning tests, where the tool was used to trace trajectories and point at marks in a rubber surface. The second set comprised manipulating sea urchin embryos both with and without the help of the tool.

A. *Positioning tests*

The ability of Micron to perform specific movement tasks was evaluated by means of a series of experiments (carried out following a board approved protocol) with three subjects having no previous experience with the system. The experiments included moving the tool tip near to laser-engraved marks on a rubber surface. The workspace was viewed by means of a 29X stereo surgical microscope (Zeiss OPMI 1). The tool was a 27 gauge hypodermic needle (400 um shaft diameter). Oblique lighting created a tool shadow depth cue (Fig. 7.)

Three tasks were performed: *hold still*, *move and hold,* and *circle tracing*. In *hold still* the tip was held over the lower right cross for 30 seconds. In *move and hold* the tip was moved to the next cross (600 um) on a tone cue, and then held for 15 seconds, repeating this operation four times. In *circle tracing* the tool was moved continuously for 60 s around the 500 um circle. There were two different test conditions: with and without cancellation (*aided* and *unaided*.) These conditions were crossed with the three task types, resulting in six different combinations.

Every subject completed six experimental sessions, which, on the basis of previous tests [10], were considered enough for the subjects to learn to use Micron. Test conditions were ordered according to a nested Latin-square

TABLE I
ERROR PERFORMANCE IN POSITIONING TASKS

Metric	Task	Unaided (um)	Aided (um)	Reduction (%)
RMS	Hold	83	51	39
	Move/hold	79	49	40
	Circle	75	49	34
Max error	Hold	260	141	46
	Move/hold	220	113	49
	Circle	311	152	51

Error reduction percentages are with respect to unaided performance.

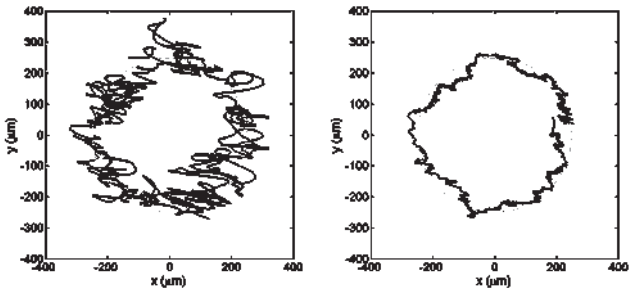

Fig. 8. Examples of trajectories followed by the tip during circle tracing tasks performed unaided and Micron-aided, respectively.

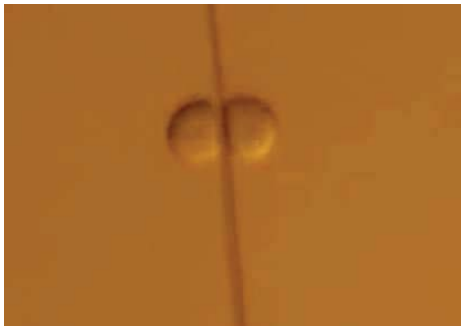
Fig. 9. Pipette held by Micron splitting sea urchin cells.

design to prevent any systematic change in performance during the experiment (due to learning or fatigue) and fatigue from affecting the results. Data from the trials were recorded at 200 Hz. Since performance converged by the fourth experiment, results from experiments 4 through 6 were pooled and analyzed by means of ANOVA.

Table I presents the results in terms of root mean square error (RMSE) and maximum error. The results obtained with the cancellation algorithm exhibited a statistically significant improvement over unaided performance; this held true for all tasks and all error metrics. Errors are calculated as 3D deviations from the target points or the circle, depending on the task. The reduction percentages shown are relative to the unaided performance. Error reduction levels are roughly similar across different tasks, falling between 34% and 40% for RMSE, and between 46% and 51% for maximum error. Figure 8 presents a sample of results. ANOVA found no relevant interaction between subject and *aided/unaided*, which suggests that the chosen filter parameters were adeqsuate for all the subjects.

B. Cell micromanipulation tests

Micron was evaluated in a sea urchin embryo cloning experiment in comparison with unaided freehand techniques. Sea urchin embryos at the 2-cell stage were placed in a 60 mm plastic dish that had been coated with 1% agarose and filled with seawater. The dish was transferred to the stage of a Zeiss M^{2}Bio stereo microscope. A sharp glass needle (which had been prepared using a Sutter horizontal pipette puller) was affixed to the Micron instrument holder. To bisect an embryo into two separate blastomeres, the dish was rotated by hand such that the long axis of the glass needle was aligned with the plane separating the two cells of the embryo. The tip of the needle was then placed in contact with the agarose near the embryo, and the needle was lowered between the two cells in a guillotine-like movement (Fig. 9) to separate the cells. Success was indicated by viability of each isolated cell (half-embryo), as determined by whether the isolated cells lysed and released cytoplasm into the medium. (Longer incubation periods showed that all cells that did not lyse immediately after the procedure subsequently underwent cell division.) Microsurgery was performed on a total of 160 embryos which were divided into 8 cohorts of 20 embryos, with 4 cohorts performed with Micron and 4 cohorts unaided. The total of cells that lysed was 2 cells with Micron, and 9 cells without.

IV. DISCUSSION

The results presented here demonstrate the general feasibility of accurate micromanipulation using a handheld tool with active error compensation. The challenge of compensating hand tremor places certain limits on the precision with which micromanipulation can be performed with Micron. While this leaves Micron at a certain disadvantage in comparison to tabletop-mounted micromanipulators, Micron also has advantages in terms of ease of use, and possibly, in the long term, low cost—advantages that perhaps may be important for certain applications.

Possible improvements of the system include reduction of the size of the manipulator, and an increase in the range of motion.

REFERENCES

[1] J. P. Desai, A. Pillarisetti, and A. D. Brooks, "Engineering approaches to biomanipulation," *Annu. Rev. Biomed. Eng.,* vol. 9, pp. 35-53, 2007.

[2] J. Voldman, "Electrical forces for microscale cell manipulation," *Annu. Rev. Biomed. Eng.,* vol. 8, pp. 425-454, 2006.

[3] G. T. Roman, Y. Chen, P. Viberg, A. H. Culbertson, and C. T. Culbertson, "Single-cell manipulation and analysis using microfluidic devices," *Anal. Bioanal. Chem.,* vol. 387, pp. 9-12, Jan 2007.

[4] M. S. Sakar, E. B. Steager, D. H. Kim, M. J. Kim, G. J. Pappas, and V. Kumar, "Single cell manipulation using ferromagnetic composite microtransporters," *Appl. Phys. Lett.,* vol. 96, Jan 25 2010.

[5] A. Ransick and E. H. Davidson, "A complete second gut induced by transplanted micromeres in the sea urchin embryo," *Science,* vol. 259, pp. 1134-1138, 1993.

[6] B. C. Becker, R. A. MacLachlan, L. A. Lobes, Jr, and C. N. Riviere, "Semiautomated intraocular laser surgery using handheld instruments," *Lasers Surg. Med.,* 2010, in press.

[7] R. A. MacLachlan and C. N. Riviere, "High-speed microscale optical tracking using digital frequency-domain multiplexing," *IEEE Trans. Instrum. Meas.,* vol. 58, pp. 1991-2001, Jun 2009.

[8] I. D. Loram, P. J. Gawthrop, and M. Lakie, "The frequency of human, manual adjustments in balancing an inverted pendulum is constrained by intrinsic physiological factors," *J. Physiol. (Lond).* vol. 577, pp. 417-432, 2006.

[9] D. Ortega Ibanez, F. P. Baquerin, D. Y. Choi, and C. N. Riviere, "Performance envelope and physiological tremor in microsurgery," in *Proc. 32nd IEEE Northeast Bioeng. Conf.*, 2006, pp. 121-122.

[10] D. Y. Choi, R. Sandoval, R. A. MacLachlan, L. Ho, L. A. Lobes, and C. N. Riviere, "Test of tracing performance with an active handheld micromanipulator," in *Proc. 29th Annu. Int. Conf. IEEE Eng. Med. Biol. Soc.*, 2007, pp. 3638-3641.